

# Weather and Forecasting

## Nonclassic Evolution of a Cold-Frontal System across the Western United States during the Intermountain Precipitation Experiment (IPEX)

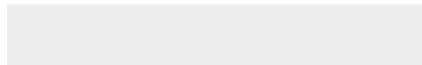
--Manuscript Draft--

<b>Manuscript Number:</b>	
<b>Full Title:</b>	Nonclassic Evolution of a Cold-Frontal System across the Western United States during the Intermountain Precipitation Experiment (IPEX)
<b>Article Type:</b>	Article
<b>Corresponding Author:</b>	David M. Schultz, Ph.D. University of Manchester Manchester, UNITED KINGDOM
<b>Corresponding Author's Institution:</b>	University of Manchester
<b>First Author:</b>	David M. Schultz, Ph.D.
<b>Order of Authors:</b>	David M. Schultz, Ph.D. W. James Steenburgh
<b>Abstract:</b>	<p>A cold-frontal passage through northern Utah was studied during Intensive Observing Period 4 of the Intermountain Precipitation Experiment (IPEX) on 14–15 February 2000. To illustrate some of its nonclassic characteristics, its origins are considered. The front developed following the landfall of two surface features on the Pacific coast (hereafter, the cold-frontal system). The first feature was a surface pressure trough and wind shift associated with a band of precipitation and rope cloud with little, if any, surface baroclinicity. The second, which made landfall 4 h later, was a wind shift associated with weaker precipitation that possessed a weak temperature drop at landfall (<math>1^{\circ}\text{C}</math> in 9 h), but developed a stronger temperature drop as it moved inland over central California (<math>4\text{--}6^{\circ}\text{C}</math> in 9 h). As the first feature moved into the Great Basin, surface temperatures ahead of the trough increased due to downslope flow and daytime heating downstream, whereas temperatures behind the trough decreased as precipitation cooled the near-surface air. As a result, this trough developed into the principal baroclinic zone of the cold-frontal system (<math>8^{\circ}\text{C}</math> in less than an hour), whereas the temperature drop with the second feature weakened further. In southeast Idaho, convection along this baroclinic zone intensified and produced a rare tornadic bow echo. The motion of the surface pressure trough was faster than the post-trough surface winds and was tied to the motion of the short-wave trough aloft. This case, along with previously published cases in the Intermountain West, challenges the traditional conceptual model of cold-frontal terminology, structure and evolution.</p>
<b>Suggested Reviewers:</b>	David Reynolds david.reynolds@NOAA.GOV  Jason Shafer jason.shafer@lyndonstate.edu  Brian Colle brian.colle@gmail.com  Howard Bluestein hblue@OU.EDU



Click here to access/download

**Cost Estimation and Agreement Worksheet  
Journals\_CEAW.pdf**



1           **Nonclassic Evolution of a Cold-Frontal**  
2           **System across the Western United States**  
3           **during the Intermountain Precipitation**  
4           **Experiment (IPEX)**

5                           DAVID M. SCHULTZ

*Centre for Atmospheric Science,*  
                          *Department of Earth and Environmental Sciences,*  
                          *University of Manchester, Manchester, United Kingdom*

                          W. JAMES STEENBURGH

*Department of Atmospheric Sciences, University of Utah, Salt Lake City, Utah*

For Submission as an Article to *Weather and Forecasting*

*Corresponding author:*

Prof. David M. Schultz, david.schultz@manchester.ac.uk

6                           August 7, 2019

## ABSTRACT

7  
8 A cold-frontal passage through northern Utah was studied during Intensive Observing  
9 Period 4 of the Intermountain Precipitation Experiment (IPEX) on 14–15 February 2000. To  
10 illustrate some of its nonclassic characteristics, its origins are considered. The front developed  
11 following the landfall of two surface features on the Pacific coast (hereafter, the cold-frontal  
12 system). The first feature was a surface pressure trough and wind shift associated with a band  
13 of precipitation and rope cloud with little, if any, surface baroclinicity. The second, which  
14 made landfall 4 h later, was a wind shift associated with weaker precipitation that possessed  
15 a weak temperature drop at landfall ( $1^{\circ}\text{C}$  in 9 h), but developed a stronger temperature drop  
16 as it moved inland over central California ( $4\text{--}6^{\circ}\text{C}$  in 9 h). As the first feature moved into the  
17 Great Basin, surface temperatures ahead of the trough increased due to downslope flow and  
18 daytime heating, whereas temperatures behind the trough decreased as precipitation cooled  
19 the near-surface air. As a result, this trough developed into the principal baroclinic zone  
20 of the cold-frontal system ( $8^{\circ}\text{C}$  in less than an hour), whereas the temperature drop with  
21 the second feature weakened further. In southeast Idaho, convection along this baroclinic  
22 zone intensified and produced a rare tornadic bow echo. The motion of the surface pressure  
23 trough was faster than the post-trough surface winds and was tied to the motion of the short-  
24 wave trough aloft. This case, along with previously published cases in the Intermountain  
25 West, challenges the traditional conceptual model of cold-frontal terminology, structure, and  
26 evolution.



# 27 1 Introduction

28 The conventional explanation for the movement of cold fronts is that they move by the  
29 advection of postfrontal cold air (e.g., Bjerknes 1919; Sanders 1955; Saucier 1955, p. 270;  
30 Wallace and Hobbs 1977, 116–117; Bluestein 1993, p. 259). This explanation works well for  
31 many fronts, but there are situations where this does not happen (e.g., Smith and Reeder  
32 1988). One such situation is in regions of complex terrain. Consider a cold front traveling  
33 over the Pacific Ocean and making landfall in the western United States. How does such  
34 a cold front subsequently pass through the western United States? Is it realistic to expect  
35 cold postfrontal air masses to be advected from the Pacific Ocean, across mountain ranges of  
36 2000–3000 m elevation, and through the Intermountain West? Does this postfrontal air mass  
37 retain its properties of temperature and moisture throughout its passage across this complex  
38 terrain? If the advection of the postfrontal airmass does not control the speed of motion of  
39 cold fronts, then the question of what controls frontal movement across the western United  
40 States—as well as other locations where complex terrain disrupts the lower-tropospheric  
41 frontal structure—becomes a relevant question for synoptic meteorology.

42 Further observations of fronts in the western United States show that they do not match  
43 the conventional conceptual model of fronts in the Norwegian cyclone model in other ways, as  
44 well. Fronts in the western United States may be associated with weak temperature gradients  
45 (Hess and Wagner 1948; McClain and Danielsen 1955), may be modified by the terrain-  
46 induced flow (e.g., Steenburgh and Blazek 2001; Neiman et al. 2004; West and Steenburgh  
47 2010), may possess multiple rainbands (e.g., Reynolds and Kuciauskas 1988), may have  
48 their thermodynamic structures altered through evaporating precipitation, intense prefrontal

49 surface heating, or orographic effects (e.g., Schultz and Trapp 2003; Shafer and Steenburgh  
50 2008; West and Steenburgh 2010, 2011), or may exhibit discrete propagation (Steenburgh et  
51 al. 2009). Indeed, issues with frontal analysis in the western United States were recognized  
52 by Williams (1972, p. 1) who identified the “failure of the classical Norwegian frontal model  
53 in many cases to adequately portray the synoptic situation as it exists.”

54 In this article, we present a case of a cold-frontal system that crossed the western United  
55 States. In describing this case, we were sometimes challenged by what to call features  
56 that did not fit the classic conceptual model of a cold front. Consequently, we refer to the  
57 entire structure as the *cold-frontal system* to discuss features that do not easily fit into our  
58 conceptual models, and we reserve the term *front* for a feature when the temperature gradient  
59 associated with a wind shift is quite strong (e.g., Sanders and Doswell 1995; Sanders 1999a).

60 The goal of this article is to elucidate and explain these nonclassic characteristics and to  
61 synthesize across several previously published cases the kinds of processes that affect frontal  
62 structure and intensity in the western United States. This event occurred during the field  
63 phase of the Intermountain Precipitation Experiment (IPEX), a research program designed  
64 to improve the quantitative prediction of precipitation over the Intermountain West of the  
65 United States through better understanding of the relevant physical processes (Schultz et  
66 al. 2002). Most of the previous research on IPEX was done on the third intensive observing  
67 period (IOP 3) where upstream flow blocked along the Wasatch Mountains favored precipi-  
68 tation well away from the slopes (Cox et al. 2005; Colle et al. 2005; Shafer et al. 2006). Also,  
69 the first known vertical profiles of the electric field in winter nimbostratus were measured  
70 during IOP 3, as well as during other IPEX IOPs (Rust and Trapp 2002). The cold-frontal  
71 system studied in the present article was the focus of IPEX’s fourth IOP (IOP 4) and was

72 known as the Valentine’s Day windstorm. The passage of the front through the Salt Lake  
73 Valley was studied by Schultz and Trapp (2003) who described the microscale structure and  
74 evolution of the front in northern Utah. They found that subcloud cooling through sublima-  
75 tion and evaporation intensified the front and produced a nonclassic, forward-tilting leading  
76 edge to the cold advection with height.

77 In the present article, we investigate the earlier structure and evolution of the cold-frontal  
78 system during IPEX IOP 4 as it moved eastward across the western United States from its  
79 arrival on the west coast of North America through to its arrival in Utah. Section 2 details  
80 some of the impacts of the frontal system ranging from the San Francisco Bay Area to  
81 the Front Range of the Rocky Mountains. Section 3 provides a synoptic overview of the  
82 cyclone and its attendant nonfrontal and frontal features on 14–15 February 2000. Section 4  
83 describes the structure of the cold-frontal system during its landfall and passage across  
84 California, and section 5 describes its development and evolution over the northern Great  
85 Basin and Snake River Plain. Finally, section 6 synthesizes the observations from this case  
86 with other previously published cases that challenge our conceptual models of cold fronts.

## 87 **2 Impacts of the cold-frontal system**

88 The 14–15 February 2000 cold-front system was associated with a weakening midlatitude  
89 cyclone that produced disruptive weather from California to eastern Colorado (Fig. 1). The  
90 following reports are a sample of those contained within *Storm Data* (NOAA 2000). A map  
91 of station and geographic locations used in this article is found in Fig. 2. Along the California  
92 coast near the Bay Area, heavy rain, as much as 127 mm (5 in) in 24 h, led to flash floods  
93 and mudslides that closed roads and caused over \$5 million in damage (Fig. 1). Highway 1

94 south of Big Sur was closed for several months due to washouts. Around 42,000 people lost  
95 power throughout the Bay Area, with another 2400 people losing power in North Monterey  
96 County due to fallen trees. Flights were delayed at San Francisco International Airport.

97 Across northern Nevada, the system produced strong wind gusts (Fig. 1). The Reno NWS  
98 Forecast Office reported wind gusts of  $33 \text{ m s}^{-1}$  (65 kt), and the Elko NWS Forecast Office  
99 (EKO) reported  $28 \text{ m s}^{-1}$  (63 mph). Other notable wind gusts from Remote Automated  
100 Weather Stations (RAWS) sites include Mather ( $36 \text{ m s}^{-1}$ , 81 mph) and Texas Springs ( $34$   
101  $\text{ m s}^{-1}$ , 77 mph). The strong winds destroyed a storage shed in Winnemucca (WMC) and a  
102 motel sign in Elko.

103 The winds continued to cause damage in southern Idaho where semi trucks and cars were  
104 blown off Interstate 84 and a house in Hagerman lost a roof (Fig. 1). A tree fell onto a car  
105 in Nampa, and the elderly driver was transported to the hospital where she died of a heart  
106 attack. In southeast Idaho, straight-line winds resulted in \$3.5 million in damage, over \$1  
107 million to irrigation wheel lines alone. Minidoka, Idaho, recorded state-record gusts to  $43.0$   
108  $\text{ m s}^{-1}$  (96.3 mph). Power was out at a potato-processing plant and a flour mill, idling over  
109 1000 workers for the next four days. The system spawned an intense band of convection  
110 in southeast Idaho that produced two F0 and three F1 tornadoes, the first tornadoes ever  
111 reported in Idaho in February (e.g., Schultz et al. 2002, pp. 199–200, 202; Ladue 2002).

112 In Utah, strong gusts exceeding  $26 \text{ m s}^{-1}$  (50 kt) also occurred (Fig. 2 in Schultz and  
113 Trapp 2003). In Brigham City, Utah, a 38-year-old woman was killed on her porch by a  
114 falling tree. The strong winds continued into the Front Range of the Rockies with peak  
115 gusts exceeding  $26 \text{ m s}^{-1}$  (50 kt) and as high as  $36 \text{ m s}^{-1}$  (70 kt). Two workers were injured  
116 in Holyoke, northeast Colorado, when the trusses on which they were standing collapsed

117 in the strong winds. Heavy snow also fell across the West, particularly along the northern  
118 part of the system, where up to 38 cm (15 in) fell in eastern Idaho, western Wyoming, and  
119 western Colorado.

120 In total, the swath of damage from this storm caused two deaths, dozens of injuries,  
121 power outtages affecting tens of thousands, and about \$10 million in damages documented  
122 in *Storm Data* alone.

### 123 **3 Synoptic overview**

124 To provide an overview of this damaging cyclone and attendant cold-frontal system, upper-  
125 air maps, infrared satellite imagery, and radar composites for the western United States are  
126 presented in this section. At 1200 UTC 14 February 2000, an upper-tropospheric trough  
127 lay offshore and was associated with a well-developed midlatitude cyclone (Figs. 3a,c). The  
128 700-hPa warm advection associated with the cyclone brought clouds and precipitation inland  
129 over Oregon, southern Washington, southern Idaho, and northern Utah (Figs. 3b,c). Cold  
130 advection at 700 hPa remained offshore (Fig. 3b). A comma-shaped cloud pattern accompa-  
131 nied the upper-level trough and mid-latitude cyclone, with the tail of the comma extending  
132 from the cyclone center onshore across Oregon and California ahead of the 700-hPa cold ad-  
133 vection. Hereafter, we refer to the tail of this comma as the principal cloud band associated  
134 with the cyclone.

135 Within this principal cloud band, heavy orographic precipitation was occurring in the  
136 Sierra Nevada of eastern California in the moist (i.e., the near-surface dewpoint in the  
137 Oakland sounding at 1200 UTC was 12°C) southwesterly flow (Figs. 3a–c). For example, the  
138 hourly precipitation gauge at Grass Valley Number 2 (732 m elevation; 80 km north-northeast

139 of SAC) reported 25 mm (1.0 in) in 4 h (1200–1600 UTC). Despite the heavy precipitation  
140 on the windward slopes, radar imagery (Fig. 3c) and hourly precipitation data from stations  
141 east of the Sierra Nevada (not shown) indicated little to no measurable precipitation was  
142 occurring at this time. Indeed, an unsaturated area at 700 hPa was located just downstream  
143 of the Sierra Nevada east of Reno, with a lee trough immediately downstream of the southern  
144 Sierra Nevada (Figs. 3b,c).

145 At 1800 UTC, the upper-tropospheric trough approached northern California, and the  
146 850-hPa low moved onshore over Washington and Oregon (Figs. 4a,c). Also, drier tropo-  
147 spheric air from the southwest and descent in the lee of the Sierra cleared out much of the  
148 cloudiness over southern California and eastern Nevada (Figs. 4b,c). This clearing is con-  
149 sistent with 6 h of transport of dry descended air at about  $30 \text{ m s}^{-1}$  (roughly the 700-hPa  
150 wind speed), which moved the edge of the moisture to Utah. Troughing at 850 hPa with a  
151 coincident band of precipitation developed over northwest Nevada. At this time, the precip-  
152 itation band, as inferred from radar reflectivity, was strongest from approximately Reno to  
153 Winnemucca, but weakened farther north.

154 By 2100 UTC, the northern end of the band strengthened and extended to the central  
155 Idaho Mountains (Fig. 5a). However, precipitation did not penetrate downstream of the  
156 southern Sierra Nevada, typical of eastward-moving cold fronts. By 2300 UTC (Fig. 5b), the  
157 band had developed into a tornadic bow echo in southeast Idaho (Ladue 2002; Schultz et  
158 al. 2002, their Fig. 10). The event was unusual, being the only cold-season bow echo west of  
159 the Rockies in Burke and Schultz’s (2004) four-year climatology of cold-season bow echoes.  
160 Within an hour, however, the bow echo had weakened, but the precipitation band remained  
161 strong as the convection moved into the Teton Range (Fig. 6c).

162 The precipitation band evolved from being well ahead of the lower-tropospheric cold-  
163 advection at 1200 UTC 14 February to being at the leading edge of lower-tropospheric cold  
164 advection at 0000 UTC 15 February (cf. Figs. 3a,b,c and 6a,b,c). At 0000 UTC 15 February,  
165 the northern part of the band moved eastward into Wyoming and the southern part of the  
166 band stalled over northern Utah (Fig. 6c), eventually dissipating in central Utah by 1000  
167 UTC 15 February (not shown). The intensification of the convection late on 14 February  
168 built up the ridge downstream of the convection that led to the weakening of the short-wave  
169 trough as it was sheared out approaching the ridge (Fig. 6a).

170 A crucial observation is that the components of the frontal system were moving rather  
171 quickly. The surface pressure trough passed Oakland, CA, at 1200 UTC and reached Wen-  
172 dover, UT, 780 km away, at 2300 UTC. These observations indicate an average speed of 19.6  
173  $\text{m s}^{-1}$ , which is faster than the component of the near-surface post-trough winds perpendic-  
174 ular to this trough of 5–15  $\text{m s}^{-1}$  (as will be shown in the next sections). Explaining why  
175 this feature moved faster than the surface winds is key to understanding the forthcoming  
176 description of its evolution.

## 177 4 Landfall and passage across California

178 Time series from surface stations in and around northern California indicate the passage of  
179 two distinct features, labeled 1 and 2 in Fig. 7. The first feature passed through northern  
180 California around 1200–1400 UTC 14 February and was associated with the principal cloud  
181 band associated with the cyclone. This cloud band was associated with a minimum, then  
182 a strong increase, in altimeter setting with veering wind (Fig. 7). Winds over the lowest  
183 3 km at profiler sites like the Sacramento Metropolitan Air Quality Management District's

184 915-MHz wind profiler at Sacramento show that this trough was associated with the change  
185 from low-level veering to a unidirectional profile from the southwest (Fig. 8). At times, the  
186 radar imagery and precipitation amounts showed an embedded line of convection with the  
187 heaviest precipitation occurring at this time (Fig. 3c). For example, Sacramento Executive  
188 Airport (SAC) received 21 mm (0.82 in) of precipitation in 5 h with this feature (Fig. 7).  
189 The surface temperature with the passage of this feature, however, only dropped 1–2°C at  
190 many stations, if at all (Fig. 7). This vertical wind-shift line through the lowest 2 km is  
191 reminiscent of some of the features associated with landfalling frontal systems in Neiman et  
192 al. (2004, their Fig. 7) with the near-vertical boundary through the lowest 300 hPa (although  
193 their front was associated with the principal temperature drop of 2°C within about 20 min;  
194 their Fig. 8).

195 A second feature passed through northern California 4–6 h later. It passed the Monterey  
196 buoy 46042 between 1600–1700 UTC, featuring a slow drop in temperature (1°C in 9 h), rise  
197 in pressure (5.8 hPa in 6 h), and veering of the wind (30° in one hour) (Fig. 7). Farther inland  
198 and after sunrise, however, the temperature drop was more sharply defined. At stations like  
199 Oakland (OAK), McClelland (MCC), Sacramento (SAC), and Stockton (SCK) (locations in  
200 Fig. 2), this feature passed around 1800–1900 UTC when the temperature dropped about  
201 4–6°C in an hour or two, and the rising pressure, which followed the first feature, began to  
202 level off (Figs. 7). The winds from the Sacramento wind profiler veered with time with the  
203 passage of the second feature from southwest to west-southwest at elevations less than about  
204 1250 m (Fig. 8). This second feature was associated with a 200-km-long line of reflectivity,  
205 which had moved to near Reno by 2100 UTC (Fig. 5a). This precipitation band had warmer  
206 cloud tops and produced less precipitation than the first band (Figs. 6c and 7). For example,



207 SAC received only 0.25 mm (0.01 in) with this band (Fig. 7).

208 Visible satellite imagery helps to distinguish these two features further. At 1800 UTC,  
209 when the principal cloud band and its associated precipitation were reorganizing in the lee of  
210 the Sierra in western Nevada and southeastern Oregon (to be discussed further in section 5),  
211 the principal cloud band was continuous with a rope cloud over the Pacific Ocean (Fig. 9a).  
212 Because of the limited availability of visible imagery early in the morning, this rope cloud can  
213 be extrapolated back to northern California around 1200 UTC, when the first feature passed  
214 through northern California. After 1800 UTC, some of the stratocumulus clouds ahead of the  
215 rope cloud dissipated (cf. Figs. 9a,b), likely indicating subsidence. This structure is hinted  
216 at in the time series from the Monterey buoy 46042, which shows decreasing dewpoint 2–6  
217 h prior to trough passage (Fig. 7).

218 The second feature entered the San Francisco Bay Area at 1800 UTC (Fig. 9a). Clouds  
219 were loosely organizing over the ocean along the secondary feature (Fig. 9a), indicating some  
220 surface convergence, which can be inferred by the wind shift in station time series (Fig. 7).  
221 But, apparently, this feature did not organize sufficiently to develop into a rope cloud as the  
222 first feature did (Fig. 9b).

223 To summarize IPEX IOP 4 over northern California, its structure was characterized by  
224 two features. The first feature was associated with the principal cloud band associated  
225 with the cyclone. Infrared satellite imagery indicated the clouds were deep, with heavy  
226 precipitation measured at the surface during the passage of this feature. Over the ocean,  
227 this feature was coincident with a rope cloud, which usually represents lower-tropospheric  
228 convergence and the leading edge of a surface front (e.g., Shaughnessy and Wann 1973; Janes  
229 et al. 1976; Woods 1983; Seitter and Muench 1985; Shapiro et al. 1985; Shapiro and Keyser

230 1990, section 10.3.1). In this case, however, the surface temperature change and wind shift  
231 were generally small, so we choose not to call this feature a front, in agreement with Sanders  
232 and Doswell (1995) and Sanders (1999a), who argued for the primacy of temperature in  
233 frontal analysis. Instead, we refer to this first feature as a surface pressure trough, as that  
234 is its key defining characteristic.

235 The second feature, on the other hand, was associated with relatively modest satellite and  
236 radar signatures. Precipitation was light. The temperature fall associated with the passage  
237 of this feature, however, was larger than with the first feature. Because the structure of these  
238 features does not fit conveniently into the terminology of the Norwegian cyclone model (e.g.,  
239 Bjerknes 1919), we refer to both the two features together by the term *cold-frontal system*.

## 240 **5 Passage across Nevada and western Utah: Frontoge-** 241 **nesis**

242 Having documented the structure of this frontal system in California, its evolution as it  
243 moved into the lee of the Sierra Nevada is examined in this section. As Fig. 7 showed,  
244 stations west of the Sierra Nevada generally presented a consistent picture of the cyclone  
245 structure with two features comprising the frontal system. On the other side of the Sierra,  
246 however, the structure of the frontal system had changed.

247 The time series from Reno (RNO) looked qualitatively similar to those from California  
248 with the passage of the first feature (i.e., surface pressure trough) at 1500 UTC, followed by  
249 the passage of the second feature at 2000 UTC (cf. Figs. 7 and 10). As with the California  
250 stations, more precipitation fell at RNO with the surface pressure trough. Within 135 km  
251 to the east, however, a dramatic change took place. Specifically, the largest temperature

252 drop at Lovelock (LOL) occurred at 1800–1900 UTC ( $7^{\circ}\text{C}$ ), consistent with the passage of  
253 the first feature (Fig. 10). The second feature weakened, becoming associated with a much  
254 slower rate of decrease in temperature ( $5^{\circ}\text{C}$  over 3 h). Indeed, Fallon Naval Air Station (not  
255 shown), only 100 km to the northeast of RNO, also showed similar features to that of LOL.

256 Thus, by the time the frontal system had moved past RNO, the trough had developed  
257 the primary baroclinicity for the cold-frontal system shortly after sunrise. In addition, the  
258 temperature fall intensified substantially to about  $8^{\circ}\text{C}$  within an hour. After passing east  
259 of RNO, precipitation was only reported with the trough. For example, LOL and EKO  
260 received only 2.5 mm (0.1 in) of precipitation each, precipitation that fell within an hour of  
261 the principal fall in temperature.

262 To understand the reasons for this change in structure of the cold-frontal system, we list  
263 the following pieces of evidence.

264 1. The surface pressure trough appeared to pass across the Sierra Nevada relatively unim-  
265 peded. A time series of stations in Nevada and western Utah shows the pressure  
266 minimum progressively moving from west to east, followed by a strong pressure rise  
267 (Fig. 10). This surface pressure trough was likely the 850-hPa trough in Fig. 4c and ap-  
268 peared to be related to forcing for surface pressure falls associated with the upper-level  
269 short-wave trough (Fig. 4a).

270 2. At some stations, downsloping winds may have cleared the skies and enhanced the  
271 temperature increase ahead of the frontal system. The warming was likely enhanced  
272 by downslope warming in the lee of the Sierra Nevada, as discussed for a different case  
273 in West and Steenburgh (2011). On a smaller scale, Wendover, UT, (ENV) on the

274 Nevada–Utah border, experienced exceptional warming and a decrease in dewpoint  
275 when the winds shifted out of the southwest at 2000 UTC and was downsloping off the  
276 adjacent Toano Mountain Range, perhaps also aided by mixing out of the overnight  
277 cold pool (Fig. 10).

278 3. Right before passage of the first feature, the temperatures rose, with the largest rises  
279 occurring at the easternmost stations in Nevada. This temperature rise was partly due  
280 to daytime heating from the clear skies ahead of the cloud band across much of Nevada  
281 (Figs. 4c and 9a), which explains why the temperature rises occurred only after sunrise  
282 and were largest at the easternmost stations in Nevada, which had the longest time  
283 to be heated. Because the air ahead of the first feature was warmed, the temperature  
284 drop associated with the frontal system increased. These high temperatures were above  
285 normal for this time of year, which also indicated the warmth of the air in the ridge  
286 ahead of the trough. For example, the daily high temperature in EKO was about  
287 12°C before passage of the first feature (Fig. 10), which is 7°C above its average high  
288 temperature for February.

289 4. The subsequent temperature drop associated with the first feature, however, only lasted  
290 a few hours. By 1900 UTC, temperatures in western Nevada had dropped by as much as  
291 7.8°C with the winds from the southwest or west (Fig. 10). By 2000 UTC, temperatures  
292 in western Nevada had recovered about 2.8°C, which in another hour returned to nearly  
293 their original temperature before the passage of the first feature.

294 5. The lower-tropospheric dewpoint depression (the difference between the air temper-  
295 ature and the dewpoint temperature) ahead of the first feature was much greater in

296 Nevada (dewpoints about 3°C and dewpoint depressions as much as 12°C) than in Cal-  
297 ifornia (dewpoints about 12°C in the Central Valley and dewpoint depressions about  
298 5°C). In other words, the lower troposphere was drier in Nevada and further from  
299 saturation.

300 6. After passing over the Sierra Nevada into Nevada, most of the precipitation associated  
301 with the frontal system was occurring at and west of the first feature (i.e., the trough).  
302 Thus, precipitation falling into the subsaturated subcloud air in Nevada led to evapo-  
303 rative cooling, which enhanced the temperature gradient, as indicated by cooling (and  
304 moistening) with the passage of the first feature at LOL, WMC, and ENV (Fig. 10).

305 7. After passage of the first feature, the pressure and dewpoint rose (Fig. 10), consistent  
306 with the creation of a mesohigh due to evaporation from precipitation aloft (e.g.,  
307 Johnson 2001; Schultz and Trapp 2003). After the temperature rebounded, many  
308 stations in Nevada experienced a continued decline in temperature over time. At  
309 EKO and ENV, the wind shift associated with this second feature became much more  
310 dramatic, with post-feature westerlies and northwesterlies.

311 These observations depict the changes to the frontal system as it moved across the Sierra  
312 Nevada and into Nevada. The surface pressure trough advanced eastward in association with  
313 a short-wave trough aloft. Precipitation formed in association with this trough evaporated  
314 into the subcloud dry air, leading to cooling behind the first feature, contributing toward  
315 the main temperature gradient developing in conjunction with the first feature. Rising  
316 temperatures east of the first feature due to downslope warming and daytime heating further  
317 increased the temperature gradient across the first feature. Confluence in the lee of the Sierra

318 Nevada (Fig. 4c) tightened the gradient of isotherms ahead of its prior location, leading to  
319 further frontogenesis. In this manner, the principal temperature drop associated with this  
320 cold-frontal system jumped from being associated with the second feature to the first feature,  
321 resembling a process of discrete frontal propagation (Charney and Fritsch 1999; Bryan and  
322 Fritsch 2000a,b; Steenburgh et al. 2009; West and Steenburgh 2010, 2011).

## 323 **6 Synthesis**

324 The characteristics of the cold-frontal system in IPEX IOP 4 bear similarities to previously  
325 documented fronts, and these characteristics have implications for conceptual models of cold  
326 fronts in the western United States, challenging the convention of a traditional cold front.  
327 This section summarizes this case by identifying its nonclassic characteristics in section 6a,  
328 comparing the frontogenesis of this case to that of other cases in section 6b, explaining the  
329 climatology of strong cold-frontal passages in section 6c, and concluding in section 6d.

### 330 **6a IPEX IOP 4: A nonclassic cold-frontal system**

331 Synthesizing these observations of the frontal system from offshore of California to its arrival  
332 in Utah, we suggest that its evolution occurred in ways that are inconsistent with traditional  
333 models of cold fronts.

#### 334 **A rope cloud did not represent the location of the strongest temperature decrease.**

335 The first feature of the frontal system possessed a rope cloud over the ocean, ahead of  
336 the line with the larger temperature drop and more modest radar and satellite signa-  
337 tures. Conventional wisdom is that a rope cloud represents the location of the surface  
338 cold front (e.g., Shaughnessy and Wann 1973; Janes et al. 1976; Woods 1983; Seit-

339 ter and Muench 1985; Shapiro et al. 1985; Shapiro and Keyser 1990, section 10.3.1).  
340 Thus, having a rope cloud along a trough without a strong temperature gradient chal-  
341 lenges our notion of what these features may represent in some cases. Although rope  
342 clouds may be associated with strong convergence, they may not be associated with  
343 the strongest baroclinicity, as shown in this present case.

344 **The landfalling cold-frontal system comprised multiple features.** This frontal sys-  
345 tem at landfall was associated with a surface pressure trough ahead of the second  
346 feature that had the larger temperature decrease (although still weak in an absolute  
347 sense). This kind of complexity of multiple features associated with frontal systems  
348 has been observed in other cases of landfalling Pacific frontal systems (e.g., Neiman  
349 et al. 2004) and beyond. For example, Schultz (2005) documented ten different types  
350 of prefrontal troughs and wind shifts associated with cold fronts. In other examples,  
351 multiple cold and warm fronts within extratropical cyclones have been documented  
352 over the North Atlantic Ocean on the Met Office surface charts (Mulqueen and Schultz  
353 2015) and over the eastern United States (Metz et al. 2005). All of these examples  
354 of cyclones with multiple features comprising frontal systems differ from the classic  
355 conceptual model of cyclones and fronts.

356 **Temperature decreases associated with the features in California were relatively weak.**

357 Although the temperature decreases associated with fronts over the ocean are reduced  
358 because of the moderating influence of the underlying ocean surface, once onshore, the  
359 temperature gradient associated with the first feature in IPEX IOP 4 increased, but  
360 still remained relatively weak. In fact, the pressure trough was the most prominent

361 characteristic of this frontal system, a point noted by other authors for other cases. For  
362 example, Williams (1969, p. 27) wrote about frontal passages at Sacramento: “Tem-  
363 perature contrasts are weak across frontal zones, and pressure tendencies are the most  
364 reliable indicators of frontal passages.” McClain and Danielsen (1955) described cases  
365 with weak baroclinicity below 700 hPa and estimated that one-third of all landfalling  
366 Pacific troughs were nonfrontal.

367 **The surface pressure trough represented the short-wave trough aloft.** This mobile  
368 surface pressure trough was associated with the steady eastward motion of an upper-  
369 level trough across the western United States that brought an end to the warm ad-  
370 vection aloft and indicated the onset of cold advection. Such surface pressure troughs  
371 can help locate upper-level short-wave troughs that might otherwise be disrupted by  
372 local effects in regions of complex topography (e.g., Hess and Wagner 1948; Schultz  
373 and Doswell 2000).

374 **The cold-frontal system moved faster than the post-system wind speed.** From land-  
375 fall in California to arrival at Utah, the pressure trough associated with the frontal  
376 system traveled at about  $20 \text{ m s}^{-1}$ , a speed higher than most of the postfrontal winds.  
377 For the front to move faster than the postfrontal winds, the generation of the evapo-  
378 ratively cooled air needed to replenish the immediate postsystem air. Both the case  
379 described by Steenburgh et al. (2009) and IPEX IOP 4 have the surface front moving at  
380 the same speed as the short-wave trough aloft. The propagation of fronts (i.e., motion  
381 faster than by advection) in the western United States has been observed previously,  
382 as well. Williams (1972, p. 1) wrote “the analysis of cold fronts themselves is subject



383 to limitations,” including “the failure to move cold fronts along with the surface gra-  
384 dient, or, more precisely, with the speed of low-level winds in the cold air-mass normal  
385 to the front.” Specifically, a “check on frontal positions can be made by association  
386 with short-wave troughs as shown on upper-air charts, preferably at the 500-mb level.  
387 Cold fronts in [the] western United States usually lie in the area of positive vorticity  
388 advection ahead of a short-wave trough” (p. 2).

389 **Discrete frontal propagation occurred in the lee of the Sierra Nevada.** Although the  
390 surface pressure trough (i.e., the first feature) was associated with a band of precipi-  
391 tation in California, its temperature drop was small. Only when precipitation fell into  
392 the drier subcloud air in the lee of the Sierra Nevada did evaporation lead to stronger  
393 cooling and less precipitation reaching the surface. In combination with downslope  
394 warming and solar heating ahead of the trough, the temperature gradient across the  
395 trough intensified, eventually becoming the dominant baroclinic zone in the frontal sys-  
396 tem. That the cooling (and moistening) lasted for only a few hours is consistent with  
397 a locally generated source of cold air, rather than postfrontal advection (e.g., Schultz  
398 and Trapp 2003). This evolution of the frontal system is reminiscent of the discrete  
399 frontal propagation described by Charney and Fritsch (1999) and Bryan and Fritsch  
400 (2000a,b), but applied to frontal movement across the Sierra Nevada by Steenburgh et  
401 al. (2009) and West and Steenburgh (2010, 2011).

402 **Subcloud evaporation was already altering the frontal structure in Nevada.** As the  
403 front moved into northern Utah, Schultz and Trapp (2003) described its structure due  
404 to subcloud evaporation and sublimation of precipitation. The subcloud dry air and

405 evaporation of subcloud precipitation was in part responsible for the formation of mam-  
406 matus on the underside of the clouds associated with the front (Schultz et al. 2006,  
407 2418–2420), indicating a cloudy layer atop a dry subcloud layer (Kanak et al. 2008).  
408 What our analysis of this event shows is that the alteration of the frontal structure by  
409 diabatic cooling had already been underway for 6 h, starting shortly after crossing the  
410 Sierra Nevada.

## 411 **6b Comparison to other cases**

412 In IPEX IOP 4, a number of processes led to the intensification of the temperature gradient  
413 across the first feature (i.e., the surface pressure trough). For example, warming downslope  
414 flow cleared clouds and allowed sensible daytime heating ahead of the surface pressure trough.  
415 Behind the trough, subcloud evaporation or sublimation cooled the lower troposphere, fur-  
416 ther enhancing the temperature difference. Such temperature differences across fronts can  
417 lead to cross-frontal circulations that intensify them further (e.g., Koch et al. 1995), at least  
418 for a short time (e.g., Sanders 1999b).

419 Once created, such temperature differences across fronts can be intensified by confluence  
420 of air masses in the lee of the Sierra Nevada. The magnitude of this confluence is likely related  
421 to the upper-level forcing as it moves through the Intermountain West. When a number of  
422 different cases of cyclone evolution through the West are examined, a key difference between  
423 these cases is the latitude, intensity, and orientation of the upper-level trough, affecting the  
424 magnitude of the confluence in the lee of the Sierra Nevada.

- 425 1. Sanders (1999b) studied an upper-level short-wave trough associated with a surface  
426 front across the southwest United States that lasted for about 18 h and was associated

427 with the strongest temperature gradient during diurnal heating. The importance of the  
428 diabatic heating ahead of the front is similar to the intensification of the frontal system  
429 in Nevada during IPEX IOP 4. However, no substantial cooling due to evaporating  
430 precipitation occurred behind the front in Sanders’s case (e.g., Sanders 1999b, his  
431 Fig. 5b and p. 2402).

432 2. West and Steenburgh (2010) examined a persistent case of confluence downstream of  
433 the Sierra Nevada that also featured intense Intermountain cyclogenesis during the Tax  
434 Day Storm. The short-wave trough was compact and intense, with the strongest forcing  
435 for pressure falls (related to the highest pressures on the dynamic tropopause) south  
436 of Lake Tahoe. The resulting 850-hPa low-pressure center was well defined with strong  
437 troughing and cyclogenesis (West and Steenburgh 2010, their Fig. 9a). The confluence  
438 served as the locus for the frontogenesis (i.e., the “collector of fronts” as described  
439 by Petterssen 1940, p. 255, and discussed by Cohen and Schultz 2005, p. 1359), but  
440 differential diabatic processes were also important for frontal development. In West  
441 and Steenburgh (2010), confluence, sensible heating, and postfrontal subcloud cooling  
442 were all important to the resulting frontogenesis.

443 3. Steenburgh et al. (2009) and West and Steenburgh (2011) examined another case (25  
444 March 2006) which featured a transient frontal system and discrete propagation. In this  
445 case, the trough was more mobile and more negatively tilted, with the strongest forcing  
446 for surface pressure falls north of Lake Tahoe. In this case, confluence frontogenesis was  
447 essential for the development and discrete propagation of the front, with differential  
448 diabatic heating contributing to the intensity of the front.

449 4. The strongest forcing in IPEX IOP4 tracks even farther north (over Oregon) compared  
450 to these previous cases, and no surface cyclone is present over the West (Fig. 6c).  
451 Without a surface cyclone, lee-side confluence is weaker and contributes less to the  
452 development and intensification of the front than in the cases described by Steenburgh  
453 et al. (2009) and West and Steenburgh (2010, 2011). In IPEX IOP 4, downslope warm-  
454 ing, sensible heating, and postfrontal subcloud cooling appeared to be most important,  
455 with confluence of secondary importance.

456 Synthesizing this case with others in the literature confirms the variety of ways that the  
457 temperature gradient and the forcing for surface pressure falls can lead to different structures  
458 and evolutions. Thus, the variety in the structure and evolution of these cases is determined  
459 by the relative importance of these various processes to frontogenesis in the Intermountain  
460 West.

## 461 **6c Explaining the climatology of strong cold-frontal passages**

462 This case—as well as previously published cases—helps to explain the climatology of strong  
463 cold-frontal passages in the western United States by Shafer and Steenburgh (2008). They  
464 defined a strong cold-frontal passage as “1) a surface temperature fall of at least 7°C over a  
465 2–3-h period, 2) a corresponding altimeter pressure rise of at least 3 hPa, and 3) the presence  
466 of a 700-hPa temperature gradient of at least 6°C (500 km)<sup>-1</sup>” (Shafer and Steenburgh 2008,  
467 p. 786). They found a large gradient in the frequency of strong cold-frontal passages across  
468 the western United States (Fig. 11). Strong cold-frontal passages are at a minimum along  
469 the Pacific coast where the influence of mild ocean air limits the formation of strong cold  
470 fronts (0–3 events over the 25-yr period 1979–2003). In contrast, a maximum in frontal

471 passages lies immediately east of the Front Range of the Rockies (150–300 events over 25  
472 yr), where strong cold fronts typically arise from cold air associated with the equatorward  
473 movement of polar anticyclones meeting warmer air from the Gulf of Mexico (e.g., Dallavalle  
474 and Bosart 1975; Rogers and Rohli 1991; Mecikalski and Tilley 1992; Schultz et al. 1997,  
475 1998). The Rockies generally block the movement of such shallow Arctic air from making it  
476 to the Intermountain West, limiting strong cold-frontal passages from this direction.

477 The Intermountain West can also be visited by strong cold fronts (10–100 events over  
478 25 yr), with the number of frontal passages increasing from west to east across central  
479 Nevada and eastern Oregon, reaching the local maximum at Salt Lake City in northern  
480 Utah (Fig. 11). This increase in frontal passages happens due to both diabatic processes  
481 (e.g., surface diurnal heating in the warm air, evaporation of precipitation in the cold air)  
482 and frontogenesis associated with confluence in the lee of the Sierra. Both of these processes  
483 would favor an increasing frequency of strong frontal passages away from the lee of the Sierra.

## 484 **6d Conclusion**

485 The observations of the cold-frontal system in this article challenge the conceptual models  
486 of cold fronts. As with other cases in the literature, the frontal system in IPEX IOP 4 was  
487 not a classic cold front as would be found in a textbook. The frontal system was composed  
488 of two features. A rope cloud was associated with a convergence line, not the principal  
489 region of baroclinicity. The surface pressure trough, tied to the short-wave trough aloft,  
490 moved faster than the winds behind it, resulting in a form of discrete frontal propagation  
491 due to the replenishment of the cold air from aloft due to evaporative cooling ahead of  
492 the frontal system. The discrete propagation of the front also addresses the question that

493 the near-surface postfrontal air that makes landfall on the California coast is not the same  
494 postfrontal air in Nevada and Utah. That air would have to be diabatically modified in situ  
495 from air with dramatically different origins. If the postfrontal air mass is not responsible  
496 for the motion of the cold front, then the conventional explanation for how cold fronts move  
497 in regions of complex terrain becomes a relevant question for synoptic meteorology. Thus,  
498 we conclude by presenting another case in which the diabatic processes (both evaporative  
499 cooling and sensible heating) and the influence of the Sierra Nevada contribute to frontal  
500 intensification and discrete propagation.

501 *Acknowledgments.* We have benefited considerably from discussions with and comments from  
502 Jason Shafer, John Horel, Greg West, and Colby Neuman, and Larry Dunn. Additional assis-  
503 tance and input was provided by Justin Cox and Mark Jackson. The Storm Prediction Center  
504 graciously provided access to their archives of surface and upper-air maps and data. David  
505 White provided the NOAA/ETL profiler data. Special thanks go to John Horel, Mike Splitt,  
506 Judy Pechmann, and MesoWest (Horel et al. 2002) for providing radar and surface data.  
507 Thanks also to the governmental agencies, commercial firms, and educational institutions  
508 that provide data to MesoWest and make this type of research possible. Funding for the field  
509 phase of IPEX was provided by the NOAA National Severe Storms Laboratory Director’s  
510 Discretionary Fund, NOAA Cooperative Institute for Regional Prediction at the University of  
511 Utah Grants NA87WA0351 and NA97WA0227, and the Utah Department of Transportation.  
512 Much of the research on this case was performed during fall 2002 while Schultz was visiting  
513 the then Department of Meteorology at the University of Utah; their support is gratefully ac-  
514 knowledged. Partial funding for Schultz was provided by NOAA/OAR/NSSL under NOAA–

515 OU Cooperative Agreement NA17RJ1227 (1998–2006) and by the UK Natural Environment  
516 Research Council through grants NE/I005234/1, NE/I024984/1, and NE/N003918/1 (2010–  
517 2019). Partial funding for Steenburgh was provided by National Science Foundation Grants  
518 ATM-0627937 and ATM-0085318 and a series of grants from the NOAA/National Weather  
519 Service CSTAR Program. The opinions, findings, recommendations, and conclusions ex-  
520 pressed in this article are those of the authors and do not reflect the official policy or po-  
521 sition of the University of Utah, National Science Foundation, or NOAA/National Weather  
522 Service.

## REFERENCES

- 523 Benjamin, S. G., J. M. Brown, K. J. Brundage, B. E. Schwartz, T. G. Smirnova, and T.  
524 L. Smith, 1998: The operational RUC-2. *Preprints, 16th Conf. on Weather Analysis and*  
525 *Forecasting*, Phoenix, AZ, Amer. Meteor. Soc., 249–252.
- 526 Bjerknes, J., 1919: On the structure of moving cyclones. *Geophys. Publ.*, **1**(2), 1–8.
- 527 Bluestein, H. B., 1993: *Synoptic–Dynamic Meteorology in Midlatitudes. Volume II: Obser-*  
528 *vations and Theory of Weather Systems*. Oxford University Press, 594 pp.
- 529 Bryan, G. H., and J. M. Fritsch, 2000a: Discrete propagation of surface fronts in a convective  
530 environment: Observations and theory. *J. Atmos. Sci.*, **57**, 2041–2060.
- 531 Bryan, G. H., and J. M. Fritsch, 2000b: Diabatically driven discrete propagation of surface  
532 fronts: A numerical analysis. *J. Atmos. Sci.*, **57**, 2061–2079.
- 533 Burke, P. C., and D. M. Schultz, 2004: A 4-yr climatology of cold-season bow echoes over  
534 the continental United States. *Wea. Forecasting*, **19**, 1061–1074.

- 535 Charney, J. J., and J. M. Fritsch, 1999: Discrete frontal propagation in a nonconvective  
536 environment. *Mon. Wea. Rev.*, **127**, 2083–2101.
- 537 Cohen, R. A., and D. M. Schultz, 2005: Contraction rate and its relationship to frontogenesis,  
538 the Lyapunov exponent, fluid trapping, and airstream boundaries. *Mon. Wea. Rev.*, **133**,  
539 1353–1369.
- 540 Colle, B. A., J. B. Wolfe, W. J. Steenburgh, D. E. Kingsmill, J. A. Cox, and J. C. Shafer, 2005:  
541 High-resolution simulations and microphysical validation of an orographic precipitation  
542 event over the Wasatch Mountains during IPEX IOP3. *Mon. Wea. Rev.*, **133**, 2947–2971.
- 543 Cox, J. A., W. J. Steenburgh, D. E. Kingsmill, J. C. Shafer, B. A. Colle, O. Bousquet, B. F.  
544 Smull, and H. Cai, 2005: The kinematic structure of a Wasatch Mountain winter storm  
545 during IPEX IOP3. *Mon. Wea. Rev.*, **133**, 521–542.
- 546 Dallavalle, J. P., and L. F. Bosart, 1975: A synoptic investigation of anticyclogenesis accom-  
547 panying North American polar air outbreaks. *Mon. Wea. Rev.*, **103**, 941–957.
- 548 Hess, S. L., and H. Wagner, 1948: Atmospheric waves in the northwestern United States. *J.*  
549 *Meteor.*, **5**, 1–19.
- 550 Horel, J., M. Splitt, L. Dunn, J. Pechmann, B. White, C. Ciliberti, S. Lazarus, J. Slemmer,  
551 D. Zaff, and J. Burks, 2002: MesoWest: Cooperative mesonets in the western United  
552 States. *Bull. Amer. Meteor. Soc.*, **83**, 211–225.
- 553 Janes, S. A., H. W. Brandli, and J. W. Orndorff, 1976: “The blue line” depicted on satellite  
554 imagery. *Mon. Wea. Rev.*, **104**, 1178–1181.
- 555 Johnson, R. H., 2001: Surface mesohighs and mesolows. *Bull. Amer. Meteor. Soc.*, **82**, 13–31.
- 556 Kanak, K. M., J. M. Straka, and D. M. Schultz, 2008: Numerical simulation of mammatus.  
557 *J. Atmos. Sci.*, **65**, 1606–1621.



- 558 Koch, S. E., J. T. McQueen, and V. M. Karyampudi, 1995: A numerical study of the effects  
559 of differential cloud cover on cold frontal structure and dynamics. *J. Atmos. Sci.*, **52**,  
560 937–964.
- 561 LaDue, J. G., 2002: The structure of a tornadic bow echo in Idaho. Preprints, *21st Conf. on*  
562 *Severe Local Storms*, San Antonio, TX, Amer. Meteor. Soc., 490–493.
- 563 McClain, E. P., and E. F. Danielsen, 1955: Zonal distribution of baroclinity for three Pacific  
564 storms. *J. Meteor.*, **12**, 314–323.
- 565 Mecikalski, J. R., and J. S. Tilley, 1992: Cold surges along the Front Range of the Rocky  
566 Mountains: Development of a classification scheme. *Meteor. Atmos. Phys.*, **48**, 249–271.
- 567 Metz, N. D., D. M. Schultz, and R. H. Johns, 2004: Extratropical cyclones with multiple  
568 warm-front-like baroclinic zones and their relationship to severe convective storms. *Wea.*  
569 *Forecasting*, **19**, 907–916.
- 570 Mulqueen, K. C., and D. M. Schultz, 2015: Non-classic extratropical cyclones on Met Office  
571 sea-level pressure charts: Double cold and warm fronts. *Weather*, **70**, 100–105,  
572 doi:10.1002/wea.2463.
- 573 Neiman, P. J., F. M. Ralph, P. O. Persson, A. B. White, D. P. Jorgensen, and D. E. Kingsmill,  
574 2004: Modification of fronts and precipitation by coastal blocking during an intense land-  
575 falling winter storm in southern California: Observations during CALJET. *Mon. Wea.*  
576 *Rev.*, **132**, 242–273.
- 577 NOAA 2000: *Storm Data*, **42**(2), 1–127.
- 578 Petterssen, S., 1940: *Weather Analysis and Forecasting*. McGraw-Hill, 505 pp.
- 579 Reynolds, D. W., and A. P. Kuciauskas, 1988: Remote and in situ observations of Sierra  
580 Nevada winter mountain clouds: Relationships between mesoscale structure, precipitation

581 and liquid water. *J. Appl. Meteor.*, **27**, 140–156.

582 Rogers, J. C., and R. V. Rohli, 1991: Florida citrus freezes and polar anticyclones in the  
583 Great Plains. *J. Climate*, **4**, 1103–1113.

584 Rust, W. D., and R. J. Trapp, 2002: Initial balloon soundings of the electric field in winter  
585 nimbostratus clouds in the USA. *Geophys. Res. Lett.*, **29**, 1959, doi:10.1029/2002GL015278.

586 Sanders, F., 1955: An investigation of the structure and dynamics of an intense surface frontal  
587 zone. *J. Meteor.*, **12**, 542–552.

588 Sanders, F., 1999a: A proposed method of surface map analysis. *Mon. Wea. Rev.*, **127**,  
589 945–955.

590 Sanders, F., 1999b: A short-lived cold front in the southwestern United States. *Mon. Wea.*  
591 *Rev.*, **127**, 2395–2403.

592 Sanders, F., and C. A. Doswell III, 1995: A case for detailed surface analysis. *Bull. Amer.*  
593 *Meteor. Soc.*, **76**, 505–521.

594 Saucier, W. J., 1955: *Principles of Meteorological Analysis*. University of Chicago Press, 438  
595 pp.

596 Schultz, D. M., 2005: A review of cold fronts with prefrontal troughs and wind shifts. *Mon.*  
597 *Wea. Rev.*, **133**, 2449–2472.

598 Schultz, D. M., and C. A. Doswell III, 2000: Analyzing and forecasting Rocky Mountain lee  
599 cyclogenesis often associated with strong winds. *Wea. Forecasting*, **15**, 152–173.

600 Schultz, D. M., W. E. Bracken, L. F. Bosart, G. J. Hakim, M. A. Bedrick, M. J. Dickinson,  
601 and K. R. Tyle, 1997: The 1993 Superstorm cold surge: Frontal structure, gap flow, and  
602 tropical impact. *Mon. Wea. Rev.*, **125**, 5–39; Corrigendum, **125**, 662.

- 603 Schultz, D. M., W. E. Bracken, and L. F. Bosart, 1998: Planetary- and synoptic-scale signa-  
604 tures associated with Central American cold surges. *Mon. Wea. Rev.*, **126**, 5–27.
- 605 Schultz, D. M., K. M. Kanak, J. M. Straka, R. J. Trapp, B. A. Gordon, D. S. Zrnić, G. H.  
606 Bryan, A. J. Durant, T. J. Garrett, P. M. Klein, and D. K. Lilly, 2006: The mysteries of  
607 mammatus clouds: Observations and formation mechanisms. *J. Atmos. Sci.*, **63**, 2409–  
608 2435.
- 609 Schultz, D. M., and R. J. Trapp, 2003: Nonclassical cold-frontal structure caused by dry sub-  
610 cloud air in northern Utah during the Intermountain Precipitation Experiment (IPEX).  
611 *Mon. Wea. Rev.*, **131**, 2222–2246.
- 612 Schultz, D. M., and coauthors, 2002: Understanding Utah winter storms: The Intermountain  
613 Precipitation Experiment. *Bull. Amer. Meteor. Soc.*, **83**, 189–210, ES1–ES31.
- 614 Seitter, K. L., and H. S. Muench, 1985: Observation of a cold front with rope cloud. *Mon.*  
615 *Wea. Rev.*, **113**, 840–848.
- 616 Shafer, J. C., and W. J. Steenburgh, 2008: Climatology of strong Intermountain cold fronts.  
617 *Mon. Wea. Rev.*, **136**, 784–807.
- 618 Shafer, J. C., W. J. Steenburgh, J. A. Cox, and J. P. Monteverdi, 2006: Terrain influences  
619 on synoptic storm structure and mesoscale precipitation distribution during IPEX IOP3.  
620 *Mon. Wea. Rev.*, **134**, 478–497.
- 621 Shapiro, M. A., and D. Keyser, 1990: Fronts, jet streams and the tropopause. *Extratropical*  
622 *Cyclones, The Erik Palmén Memorial Volume*, C. W. Newton and E. O. Holopainen,  
623 Eds., Amer. Meteor. Soc., 167–191.
- 624 Shapiro, M. A., T. Hampel, D. Rotzoll, and F. Mosher, 1985: The frontal hydraulic head: A  
625 micro- $\alpha$  scale ( $\sim 1$  km) triggering mechanism for mesoconvective weather systems. *Mon.*  
626 *Wea. Rev.*, **113**, 1166–1183.

- 627 Shaughnessy, J. E., and T. C. Wann, 1973: Frontal rope in the North Pacific. *Mon. Wea.*  
628 *Rev.*, **101**, 774–776.
- 629 Smith, R. K., and M. J. Reeder, 1988: On the movement and low-level structure of cold  
630 fronts. *Mon. Wea. Rev.*, **116**, 1927–1944.
- 631 Steenburgh, W. J., and T. R. Blazek, 2001: Topographic distortion of a cold front over the  
632 Snake River Plain and central Idaho mountains. *Wea. Forecasting*, **16**, 301–314.
- 633 Steenburgh, W. J., C. R. Neuman, G. L. West, and L. F. Bosart, 2009: Discrete frontal  
634 propagation over the Sierra–Cascade Mountains and Intermountain West. *Mon. Wea.*  
635 *Rev.*, **137**, 2000–2020.
- 636 Wallace, J. M., and P. V. Hobbs, 1977: *Atmospheric Science: An Introductory Survey*. Aca-  
637 demic Press, 467 pp.
- 638 West, G. L., and W. J. Steenburgh, 2010: Life cycle and mesoscale frontal structure of an  
639 Intermountain cyclone. *Mon. Wea. Rev.*, **138**, 2528–2545.
- 640 West, G. L., and W. J. Steenburgh, 2011: Influences of the Sierra Nevada on Intermountain  
641 cold-front evolution. *Mon. Wea. Rev.*, **139**, 3184–3207.
- 642 Williams, P., Jr., 1969: Station descriptions of local effects on synoptic weather patterns.  
643 U.S. Weather Bureau Western Region, Tech. Memo. WBTM WR-5 (Revised), 54 pp.  
644 [Available from NOAA NWS Western Region Headquarters, 125 S. State Street, Rm.  
645 1311, Salt Lake City, UT 84138-1102.]
- 646 Williams, P., Jr., 1972: Western Region synoptic analysis—Problems and methods. NOAA  
647 NWS Western Region Tech. Memo. NWSTM WR-71, 71 pp. [Available from NOAA  
648 NWS Western Region Headquarters, 125 S. State Street, Rm. 1311, Salt Lake City, UT  
649 84138-1102.]

650 Woods, V. S., 1983: Rope cloud over land. *Mon. Wea. Rev.*, **111**, 602–607.

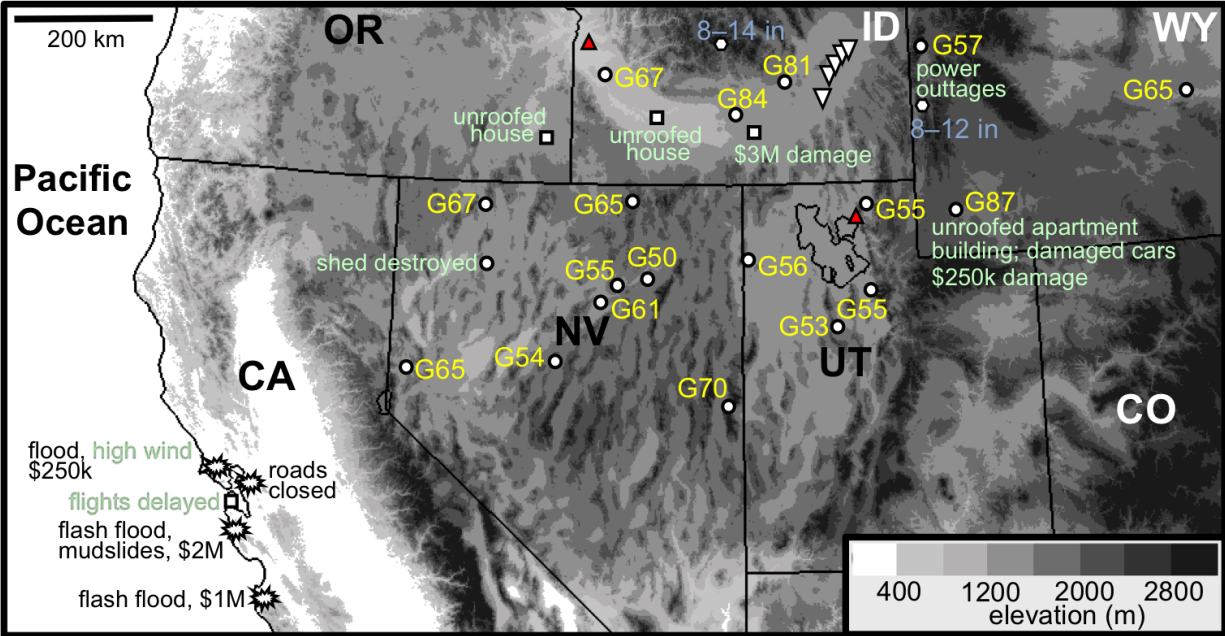


Figure 1: A selection of *Storm Data* (NOAA 2000) reports for 14 February 2000. Wind gusts (kt) are reported in yellow as GXX and are indicated by small white circles. Explosion symbols represent impacts from heavy rain and flooding, squares and green text represent impacts from strong winds, hexagons and blue text represent snowfall amounts (in), downward-pointing white triangles represent tornadoes, and upward-pointing red triangles represent deaths. Elevation above sea level is shaded every 400 m according to scale.

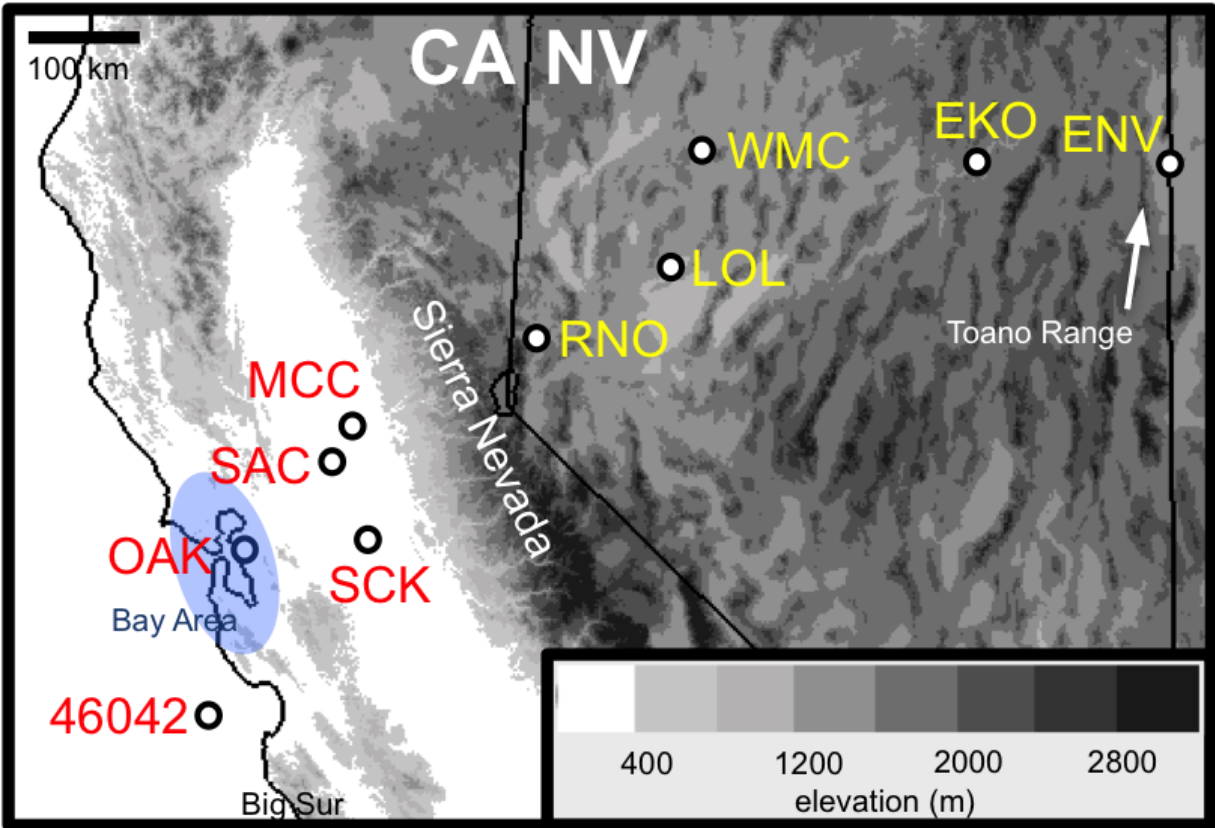


Figure 2: Station locations in time-series plots across California for Fig. 7 (labeled in red) and across Nevada for Fig. 10 (labeled in yellow): buoy 50 km west-northwest of Monterey (46042), Oakland (OAK), McClelland (MCC), Sacramento (SAC), Stockton (SCK), Reno (RNO), Lovelock (LOL), Winnemucca (WMC), Elko (EKO), and Wendover (ENV). Some geographic locations described in text are also labeled. Elevation above sea level is shaded every 400 m according to scale.

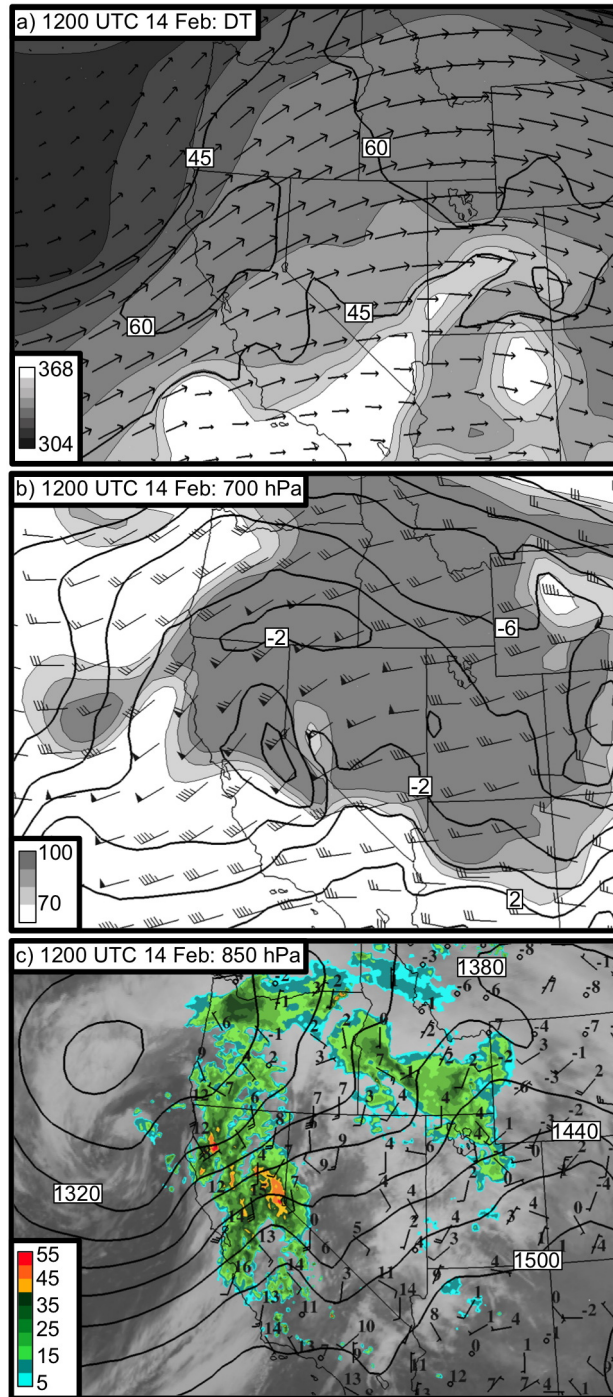


Figure 3: Regional analyses from the Rapid Update Cycle, version 2 (RUC2; Benjamin et al. 1998) at 1200 UTC 14 February 2000. (a) Dynamic-tropopause (DT) potential temperature (shaded every 8 K following inset scale), isotachs (contours at 45 and 60  $\text{m s}^{-1}$ ), and wind vectors. (b) 700-hPa temperatures (contours every  $2^{\circ}\text{C}$ ), relative humidity greater than 70% (shaded every 10% following inset scale), and wind (pennants, full barbs, and half-barbs denote 25, 5, and  $2.5 \text{ m s}^{-1}$ , respectively). (c) 850-hPa geopotential height (contours every 30 m), NEXRAD 8-km composite radar reflectivity (greater than 5 dBZ color-filled following inset scale), infrared satellite imagery, and selected MesoWest surface observations of temperature ( $^{\circ}\text{C}$ , upper right) and wind [barbs as in (b)].



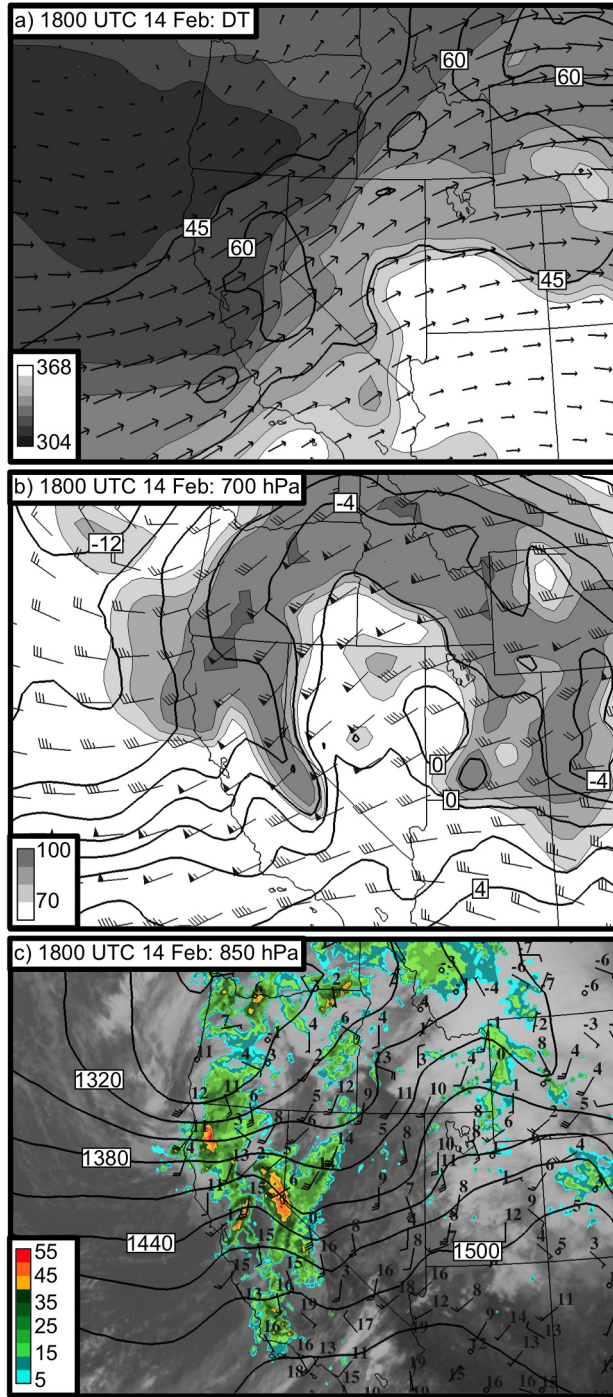


Figure 4: Regional analyses from the RUC2 at 1800 UTC 14 February 2000. (a) Dynamic-tropopause (DT) potential temperature (shaded every 8 K following inset scale), isotachs (contours at 45 and 60 m s<sup>-1</sup>), and wind vectors. (b) 700-hPa temperatures (contours every 2°C), relative humidity greater than 70% (shaded every 10% following inset scale), and wind (pennants, full barbs, and half-barbs denote 25, 5, and 2.5 m s<sup>-1</sup>, respectively). (c) 850-hPa geopotential height (contours every 30 m), NEXRAD 8-km composite radar reflectivity (greater than 5 dBZ color-filled following inset scale), infrared satellite imagery, and selected MesoWest surface observations of temperature (°C, upper right) and wind [barbs as in (b)].

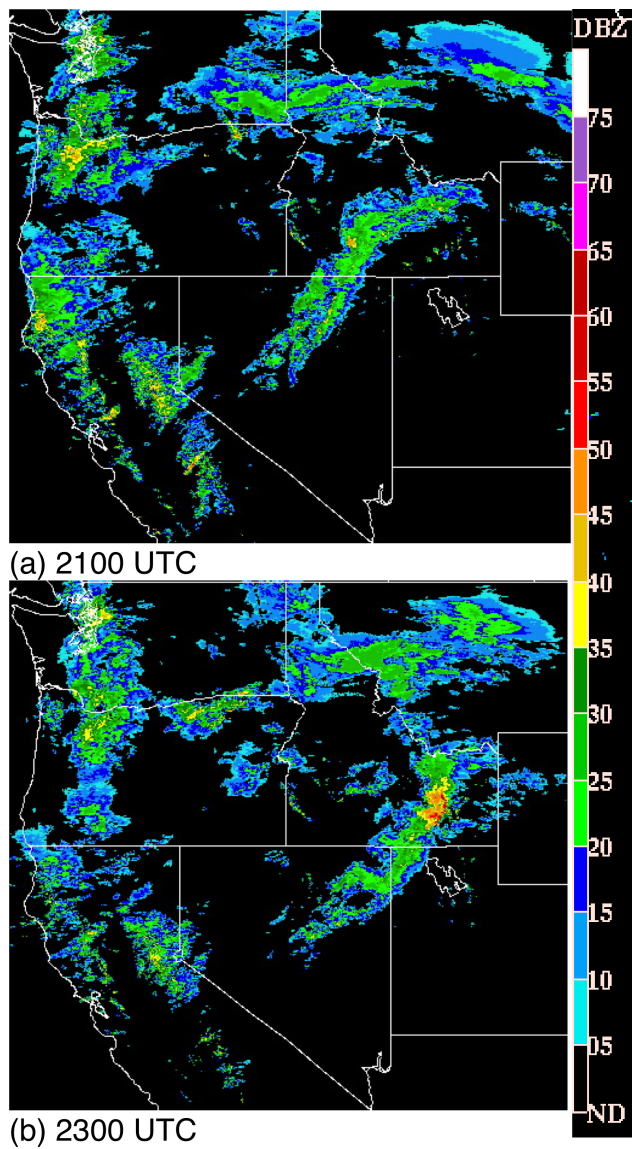


Figure 5: Radar reflectivity factor (dBZ, according to scale) for 14 February 2000: (a) 2100 UTC and (b) 2300 UTC.

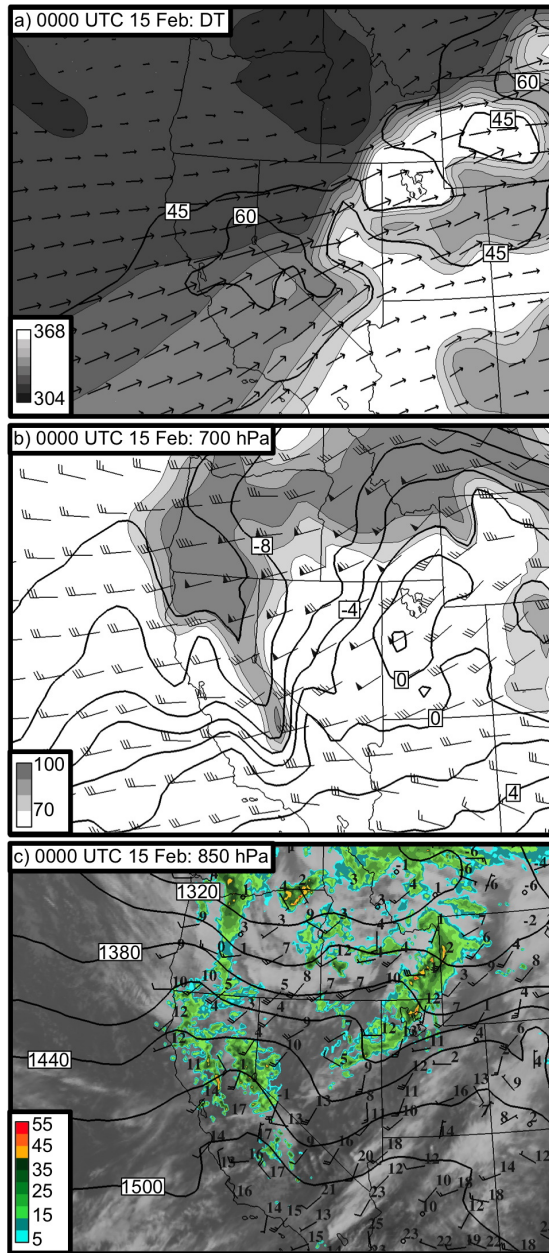


Figure 6: Regional analyses from the RUC2 at 0000 UTC 15 February 2000. (a) Dynamic-tropopause (DT) potential temperature (shaded every 8 K following inset scale), isotachs (contours at 45 and 60  $\text{m s}^{-1}$ ), and wind vectors. (b) 700-hPa temperatures (contours every 2°C), relative humidity greater than 70% (shaded every 10% following inset scale), and wind (pennants, full barbs, and half-barbs denote 25, 5, and 2.5  $\text{m s}^{-1}$ , respectively). (c) 850-hPa geopotential height (contours every 30 m), NEXRAD 8-km composite radar reflectivity (greater than 5 dBZ color-filled following inset scale), infrared satellite imagery, and selected MesoWest surface observations of temperature ( $^{\circ}\text{C}$ , upper right) and wind [barbs as in (b)].



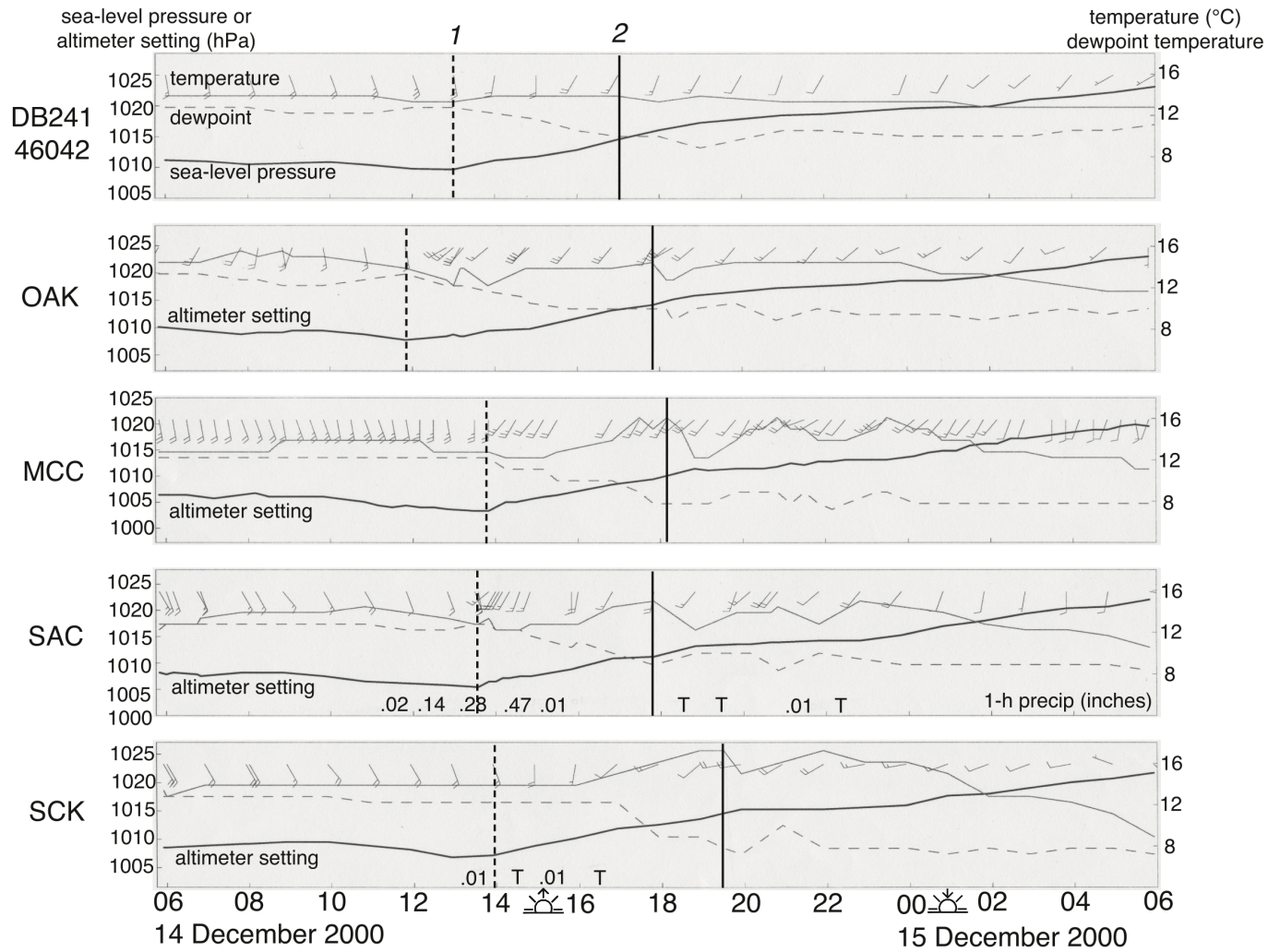


Figure 7: Meteograms from surface stations in California: buoy 50 km west-northwest of Monterey (46042), Oakland (OAK), McClelland (MCC), Sacramento (SAC), and Stockton (SCK). The dashed vertical lines labeled “1” represent the first feature (i.e., trough passage), and the solid lines labeled “2” represent the second feature. Notation for the wind is pennants, full barbs, and half-barbs denote 25, 5, and 2.5 m s<sup>-1</sup>, respectively. Icons along time axis represent sunrise (sun with up arrow) and sunset (sun with down arrow).

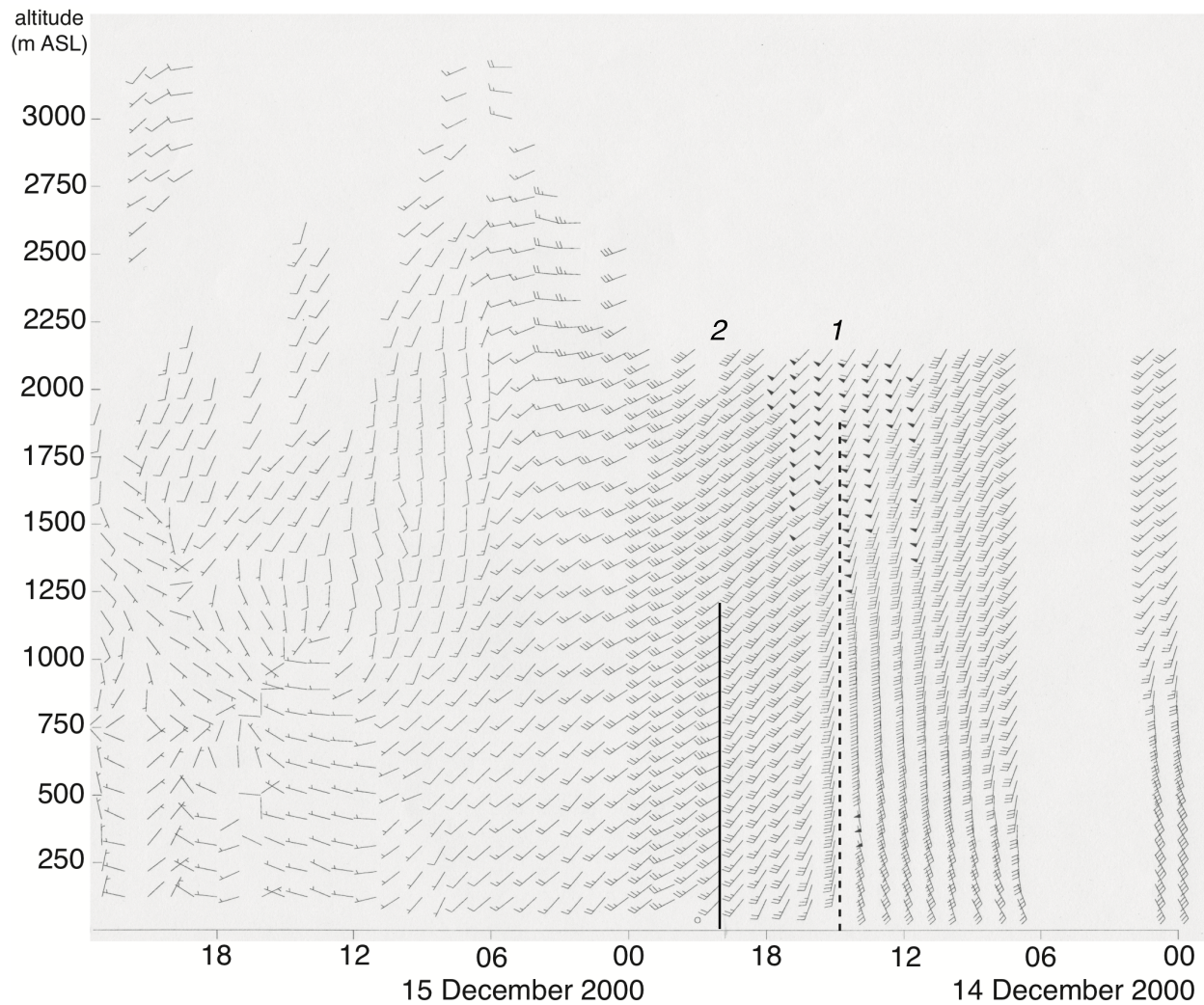


Figure 8: Time–height series of wind from the Sacramento Metropolitan Air Quality Management District’s 915-MHz wind profiler at Sacramento from 0000 UTC 14 December to 2300 UTC 15 December 2000. Notation for the wind is pennants, full barbs, and half-barbs denote 25, 5, and 2.5 m s<sup>-1</sup>, respectively. The dashed vertical line labeled “1” represents the first feature (i.e., trough passage), and the solid line labeled “2” represents the second feature.



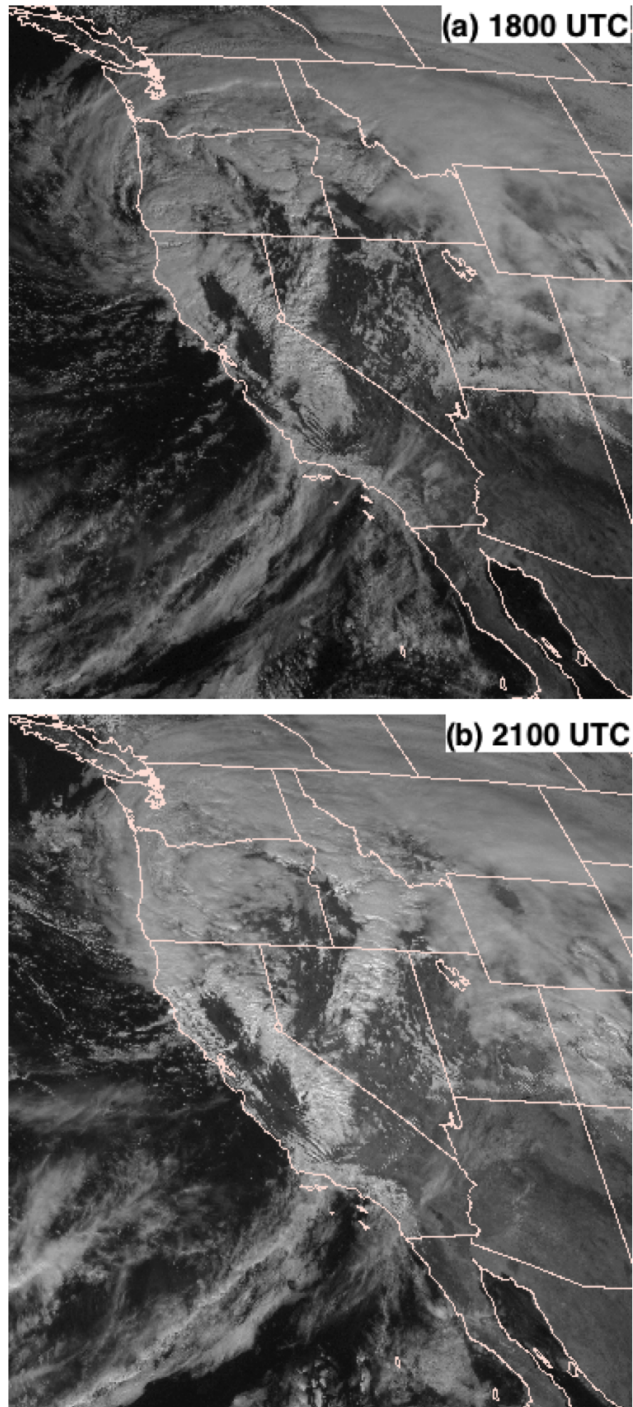


Figure 9: *GOES-10* visible satellite imagery 14 February 2000: (a) 1800 UTC and (b) 2100 UTC.

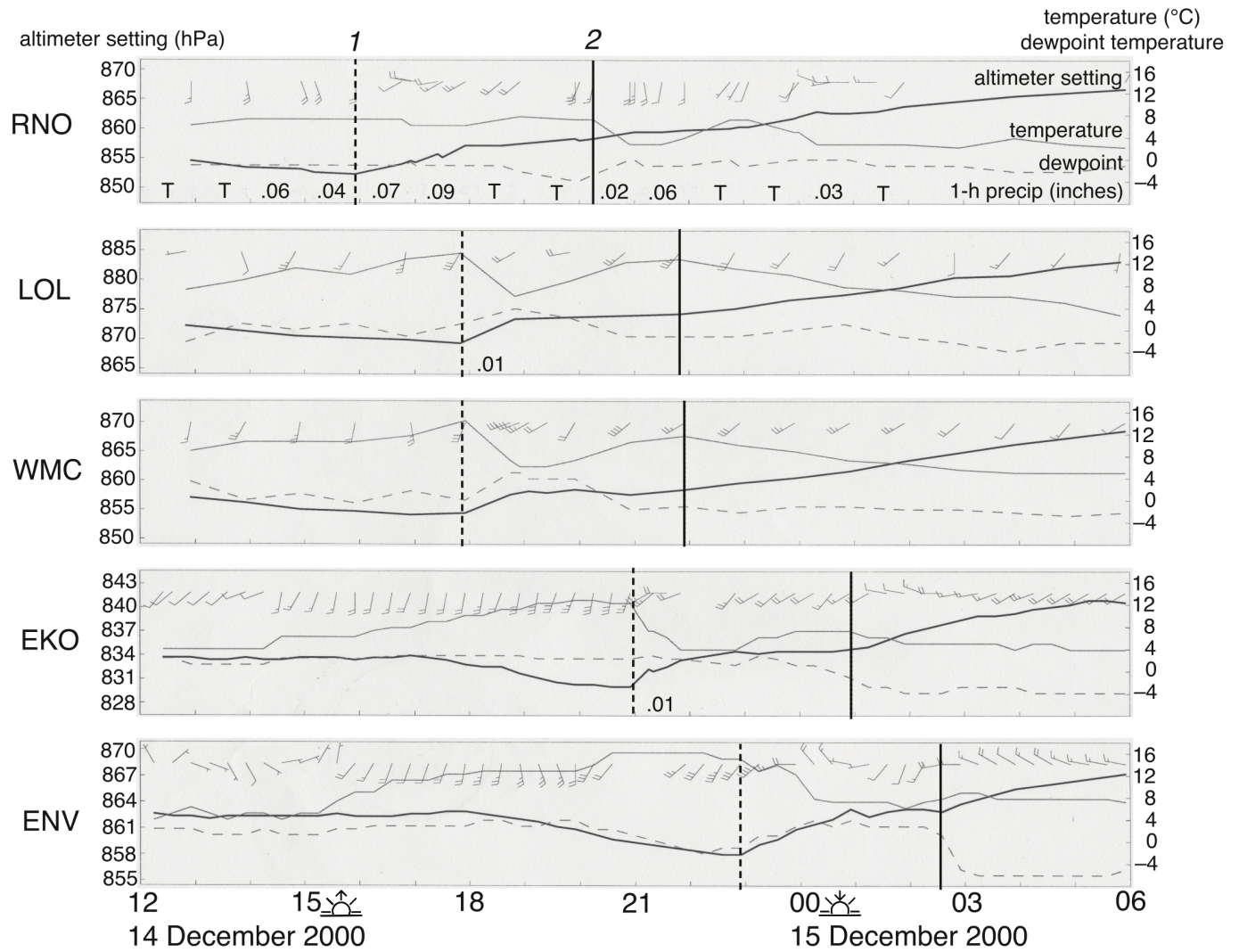


Figure 10: Meteograms from surface stations in Nevada and Utah: Reno (RNO), Lovelock (LOL), Winnemucca (WMC), Elko (EKO), and Wendover (ENV). The dashed vertical lines labeled “1” represent the first feature (i.e., trough passage), and the solid lines labeled “2” represent the second feature. Notation for the wind is pennants, full barbs, and half-barbs denote 25, 5, and 2.5 m s<sup>-1</sup>, respectively. Icons along time axis represent sunrise (sun with up arrow) and sunset (sun with down arrow).

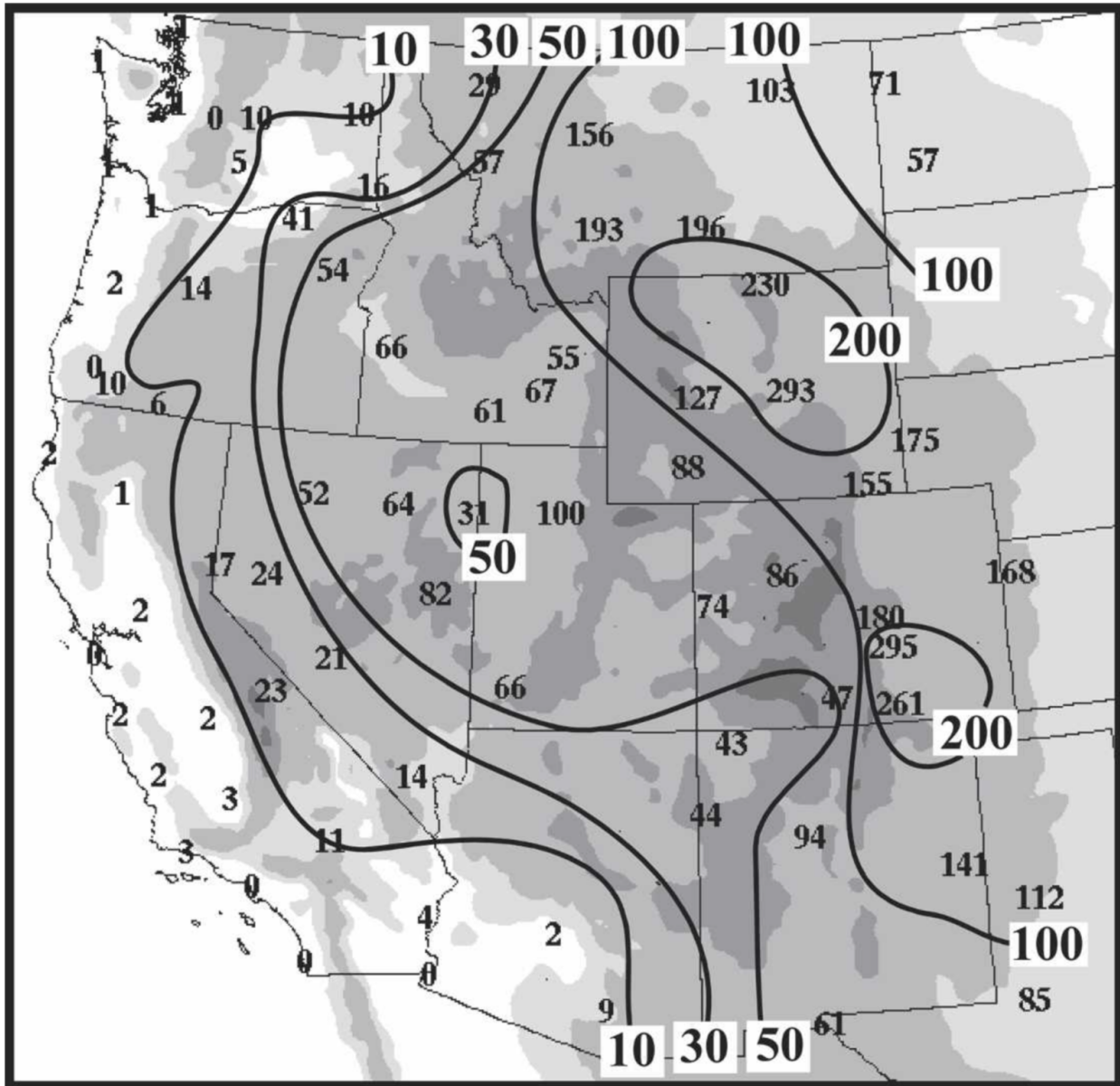


Figure 11: Total number of strong cold-frontal passages (1979–2003) with arbitrary contours. Terrain shaded at intervals of 0.5, 1, 2, and 3 km. Figure and caption adapted from Shafer and Steenburgh (2008, their Fig. 4).